Chemical Engineering Journal 149 (2009) 263–272

Contents lists available at ScienceDirect

Chemical Engineering Journal

journal homepage: www.elsevier.com/locate/cej

# Selective separation of basic and reactive dyes by molecularly imprinted polymers (MIPs)

George Z. Kyzas, Dimitrios N. Bikiaris, Nikolaos K. Lazaridis*

*Division of Chemical Technology, School of Chemistry, Aristotle University of Thessaloniki, GR-541 24 Thessaloniki, Greece*

ARTICLE INFO

*Article history:*
Received 22 July 2008
Received in revised form 20 October 2008
Accepted 3 November 2008

*Keywords:*
Molecular imprinting
Selective adsorption
Basic dyes
Reactive dyes
Isotherms
Kinetics
Real effluents

ABSTRACT

In this study, two water-compatible molecularly imprinted polymers (MIPs) were prepared for the selective adsorption of a Reactive Red (RR) and Basic Red dye (BR). The preparation of BR-MIP was carried out in organic medium, while the preparation of RR-MIP in aqueous medium. Characterization of the obtained dye—MIPs was achieved by FTIR spectra, SEM micrographs, and swelling experiments. Kinetic experiments were successfully described by the intraparticle diffusion model. Equilibrium experiments, at various temperatures, were described by the Freundlich model. The process was endothermic and could be classified as electrostatic adsorption. The effect of pH on adsorption and desorption was studied, as well as a potential adsorption/rebinding mechanism of dyes by MIPs is also proposed. The regenerability of MIPs was affirmed in four sequential cycles of adsorption/desorption, without significant loss in adsorption capacity. Selectivity experiments showed the high affinity of target molecules over competitive dyes for the respective MIPs.



## 1. Introduction

The history of molecular imprinting is traced back in 1940s and 1950s, when there was an inspiration to create affinity for dye molecules in silica gel, which is considered to be the first imprinted material [1]. Molecularly imprinted polymers (MIPs) represent a new class of materials that have artificially created receptor structures [2–5]. Since their discovery in 1972, MIPs have attracted considerable interest from scientists and engineers involved in the development of chromatographic adsorbents, membranes, sensors and enzyme and receptor mimics [6].

Dye molecules, according to their charge, can be classified as: anionic (direct, acid, reactive), cationic (basic) and nonionic (disperse). Depending upon their structure, azo- and anthraquinonic-dyes are the two major classes and together represent 90% of all organic colorants [7]. It is known that wastewaters containing dyes are very difficult to treat, since these chemicals are recalcitrant molecules resistant to traditional aerobic digestion [8]. It should be also stressed that the dyeing process is usually realized by mixture of dyes (trichromatic) to produce the various shades [9]. As a result, wastewaters originating from the dyeing reactor bear three dyes. Adsorption of dye molecules onto a sorbent can be an effective low-cost method of color removal. Activated carbon is the most commonly used method of dye removal by adsorption. Activated carbon is expensive, with high regeneration cost and 10–15% loss in the reactivation procedure [10]. MIPs specially prepared for the three dyes could be an alternative sorbent for the selective separation of each dye molecule. Moreover, desorption and possible reuse of dyes could give an important economic and environmental impetus.

This team has succeeded the preparation of sorbents with high adsorption capacity for the removal of dyes, but without achieving any selectivity [11]. In literature, it has not been extensively studied the removal/recognition of a dye molecule as template with MIPs. Only, Yan et al. tried to study the binding properties of a dye-imprinted polymer using a basic dye (malachite green) as template [12].

MIPs traditionally demonstrate their best performance in hydrophobic organic solvents, such as chloroform or toluene [13]. This could be explained by the fact that apolar solvents eliminate the non-specific hydrophobic interactions and create the best environment for electrostatic interactions which play an important role in molecular recognition [13]. Purification and solid phase extraction of natural products constitute areas for MIPs application where the use of hydrophobic solvents could give an advantage [13]. However, there are many others such as environmental analysis, which require full compatibility with water [13].

The novelty of this study is the preparation of water-compatible MIPs for the selective removal of dye molecules from trichromatic dye aqueous solutions. A reactive and a basic (both azo-dyes), were

* Corresponding author. Tel.: +32 310 997807; fax: +32 310 997859.
*E-mail address:* nlazarid@chem.auth.gr (N.K. Lazaridis).

1385-8947/$ – see front matter © 2008 Elsevier B.V. All rights reserved.
doi:10.1016/j.cej.2008.11.002

used as main templates, while other two reactive and two basic used as co-existent dyes. The rebinding properties and the adsorption capacity were demonstrated by equilibrium/rebinding batch experiments. The selectivity/specificity of the obtained materials was elucidated by performing adsorption experiments in trichromatic dye solutions. Moreover, the regeneration possibility of the dye-loaded polymers was evaluated, offering additional impetus for improved process economics.

## 2. Materials and methods

### 2.1. Materials

For synthesis of MIPs, methacrylic acid (MAA) and acrylamide (AAm) were used as monomers, ethylene glycol dimethacrylate (EGDMA) and *N*,*N*′-methylenebisacrylamide (MBA) as cross-linkers, dimethylformamide (DMF) as solvent, 2,2′-azobis(isobutyronitrile) (AIBN) and potassium persulfate (KPS) as initiators. Remazol Red 3BS (RR) ($C_{31}H_{19}ClN_7Na_5O_{19}S_6$, M.W. = 1136.31 g/mol, $\lambda_{max}$ = 588 nm, 58%, w/w), and Remacryl Red TGL (BR) ($C_{19}H_{25}Cl_2N_5O_2$, M.W. = 424.34 g/mol, $\lambda_{max}$ = 488 nm, 86%, w/w) were the template molecules. For the selectivity experiments four other dyes were used as competitive dyes; Basic Blue 3G (BB) ($C_{20}H_{26}ClN_3O$, M.W. = 359.18 g/mol, $\lambda_{max}$ = 607 nm, 53%, w/w), Basic Yellow 37 (BY) ($C_{21}H_{29}N_3$, M.W. = 323.48 g/mol, $\lambda_{max}$ = 440 nm, 55%, w/w), Remazol Blue RN (RB) ($C_{22}H_{162}Na_2O_{11}S_3$, M.W. = 626.54 g/mol, $\lambda_{max}$ = 541 nm, 56%, w/w), Remazol Yellow gelb 3RS 133% (RY) ($C_{28}H_{20}ClN_9Na_4O_{16}S_5$, M.W. = 1026.25 g/mol, $\lambda_{max}$ = 419 nm, 60%, w/w). The chemical structures of all dyes are given in Table 1. All solvents, reagents and compounds of polymerization were supplied by Sigma–Aldrich.

### 2.2. Synthesis of MIPs

For the preparation of Red Reactive dye-MIP (RR-MIP), 2 mmol AAm, 10 mmol MBA, 1 mmol Reactive Red dye (RR) and 0.185 mmol KPS were dissolved in 50 mL of water into a glass flask, while for Basic Red dye-MIP (BR-MIP) 2 mmol of MAA, 10 mmol EGDMA, 1.6 mmol Basic Red dye (BR) and 0.05 g AIBN were dissolved in 50 mL of the organic solvent DMF [14]. The functional monomer and cross-linker were determined by the ratio of 2:10 [15]. In both methods, the mixture of reagents was stirred for 2 h, followed by nitrogen sparging (∼5 min) to remove oxygen. After then, the flask was immediately sealed and stirring was continued at 75 °C for 12 h. The flask was then smashed and the monolithic polymers obtained, were ground in a laboratory mortar and pestle. Next, the obtained particles were washed with acetone and hot water, followed by extraction in a Soxhlet apparatus using methanol, in order to remove residuals of the monomers and template molecules. The extraction lasted for 16 h, a sum of 30–35 solvent cycles (each cycle lasts approximately 30 min). At the end of the 16-h period, the higher percentage of template molecules (91%) was removed from the polymer matrix, giving that for non-covalent imprinting 85–95% was reported to be the ideal range of the template extraction from the polymer [16]. Non-imprinted polymers (NIPs) were prepared with the same procedure just in the absence of the template molecules, denoted hereafter as R-NIPs and B-NIPs, respectively.

### 2.3. Characterization

The structure of the binding sites of a MIP cannot be determined either with crystallographic or microscopy methods, because of their deformity. Therefore, there are only a limited number of direct physical characterization methods for imprinted polymers. These include surface area measurements (via BET analysis), IR spectroscopy, scanning electron microscopy and swelling experiments. The spectroscopic methods are the best for investigating molecular level features of MIPs, while the surface area and swelling measurements characterize macroscopic features.

For the swelling degree measurements 0.5 g of sample was placed in 100 mL aqueous solution adjusted to pH 10 for BR-MIP and to pH 2 for RR-MIP; optimum pH values found from pH-edges experiments. After immersion for 24 h at room temperature, by which time the material has finally completed swelling (after five measurements until there was no further weight increase), the material was removed from the solvent by filtration and excess solvent was removed carefully staved off the by blotting with moist filter paper. The weight of the swollen sample was measured and the swelling degree (%) was calculated using Eq. (1):

$$S = \frac{W_s - W_0}{W_0} \cdot 100\% \quad (1)$$

where $W_s$ and $W_0$ are the weights of the swollen and dry polymer, respectively.

FTIR spectra of MIPs were obtained by a PerkinElmer FTIR spectrophotometer, model Spectrum 1000, in the range of 4000–500 $cm^{-1}$ using KBr pellets containing the prepared materials. The resolution for each spectrum was 2 $cm^{-1}$ and the number of co-added scans was 64. The spectra presented are baseline corrected and converted to the absorbance mode.

In addition, surface areas of the MIPs were determined with a Micromeritics BET (Brunauer, Emmett and Teller) surface area analyzer, model TriStar 3000, by means of adsorption of ultra pure nitrogen.

Scanning electron microscopy of the prepared particles was carried out using a JEOL JMS-840A scanning microscope equipped with an energy-dispersive X-ray (EDX) Oxford ISIS 300 micro-analytical system. All the studied surfaces were coated with carbon black to avoid charging under the electron beam.

In order to find out the $pH_{zpc}$ of the material (pH at which the materials do not induce the release of either $H^+$ or $OH^-$ ions into the solution) the solid addition method described by Balistrieri and Murray was realized [17].

### 2.4. Adsorption–desorption

#### 2.4.1. Effect of pH (pH-edges)

The influence of pH over the adsorption process was studied by mixing 0.5 g of sorbent with 50 mL of a dye solution (100 mg/L). Immediately after mixing, the suspension was allowed to bind dyes by shaking for 24 h. The temperature was maintained constant at 25 ± 1 °C using water bath (Julabo SW-21C). The pH value, ranging between 2 and 12, was kept constant throughout the adsorption process. It was found from the experimental data that the higher dye uptake was at pH 2 for RR-MIP and at pH 10 for BR-MIP. Therefore, these pH values were selected for the rebinding experiments.

#### 2.4.2. Kinetic experiments

Batch kinetic experiments were performed by mixing a fixed amount of sorbent (0.5 g) with 50 mL of a dye solution (100 mg/L). Immediately after mixing, the suspension was allowed to bind dyes by shaking for 24 h. During this period samples were collected at fixed intervals. After the spectrophotometric analysis of each sample, the concentration of dye in the aqueous solution ($C_t$) was calculated. The following intraparticle diffusion model was used in order to estimate the intraparticle diffusion coefficient, $D$ ($m^2/s$)

**Table 1**
Molecular structures of the studied dyes.

| Reactive dyes | Basic dyes |
|---|---|
| 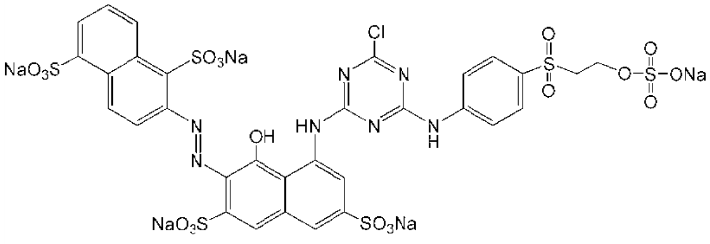 | 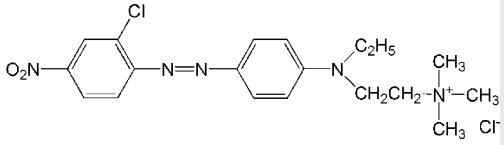 |
| Remazol Brillant Red 3BS (RR) $C_{31}H_{19}ClN_7Na_5O_{19}S_6$ | Remacryl Red TGL (BR) $C_{19}H_{25}Cl_2N_5O_2$ |
| 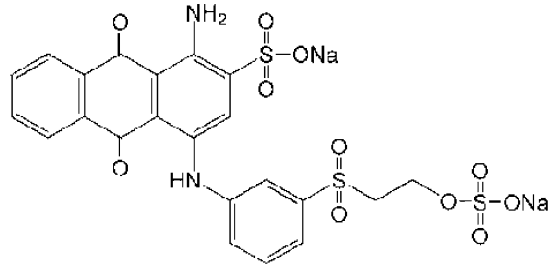 | 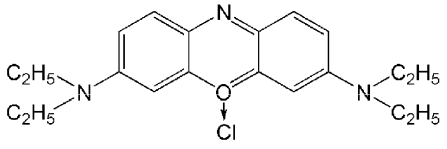 |
| Remazol Brillant Blue RN (RB) $C_{22}H_{16}N_2Na_2O_{11}S_3$ | Basic Blue 3G (BB) $C_{20}H_{26}ClN_3O$ |
| 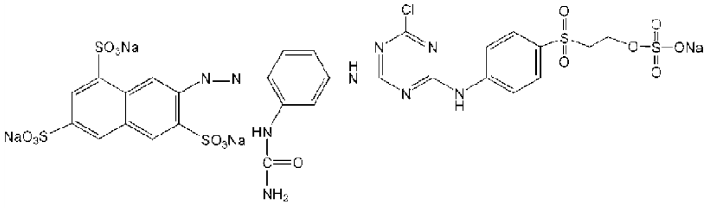 | 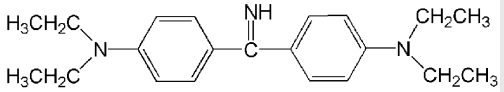 |
| Remazol Yellow Gelb 3RS (RY) $C_{28}H_{20}ClN_9Na_4O_{16}S_5$ | Basic Yellow 37 (BY) $C_{21}H_{29}N_3$ |

(Eq. (2)) [18,19]:

$$X = \frac{C_0 - C_t}{C_0 - C_e} = \left[1 - \exp\left(\frac{-4\pi Dt}{2.3d^2}\right)\right]^{1/2} \quad (2)$$

where $d$ is the particle diameter (m) and, $C_0$, $C_t$, $C_e$ are the initial, transient and equilibrium concentrations of dye in the aqueous solution (mg/L), respectively. The diffusion coefficient, which is the sum of pore and surface diffusion, can be measured from the half-time for adsorption ($X = 0.50$).

### 2.4.3. Equilibrium experiments—thermodynamics

The effect of initial dye concentration was determined by contacting 0.5 g sorbent with 50 mL of dye solutions (10–200 mg/L). Immediately after mixing, the suspension was allowed to bind dyes by shaking for 24 h (at pH 10 for BR-MIP and at pH 2 for RR-MIP). The temperature was maintained constant at $25 \pm 1\,^{\circ}C$, $45 \pm 1\,^{\circ}C$, $65 \pm 1\,^{\circ}C$. The same experiments were performed for the respective NIPs.

The Freundlich isotherm is believed to be the better equilibrium model for MIPs [20]. This model is derived by assuming a heterogeneous surface with a non-uniform distribution of heat of adsorption over the surface and is expressed by Eq. (3) [21]:

$$Q_e = K_F C_e^n \quad (3)$$

where $Q_e$ is the equilibrium dye concentration in the solid phase (mg/g); $K_F$ is the Freundlich constant representing the adsorption capacity ($mg^{(1-n)}\ L^n/g$); $n$ is a constant depicting the adsorption intensity/nonlinearity. The case $n < 1$ reflects the situation in which at higher and higher sorbate concentrations, it becomes more and more difficult to sorb additional molecules. This may occur in cases where specific binding sites become filled or remaining sites are less attractive to the sorbate molecules. The case $n > 1$ describes a contrasting situation in which previously sorbed molecules lead to a modification of the surface which favours further adsorption [22].

The Gibbs free energy change, $\Delta G^0$ (kJ/mol), of the adsorption process is related to the equilibrium constant, $K_c$, by the van't Hoff Eq. (4) [23]:

$$\Delta G^0 = -RT \ln K_c \quad (4)$$

It is also related to the change in entropy, $\Delta S^0$ (J/mol K) and the heat of adsorption, $\Delta H^0$ (kJ/mol), at a constant temperature, $T$ (K), as follows:

$$\Delta G^0 = \Delta H^0 - T\,\Delta S^0 \quad (5)$$

where $R$ is the universal gas constant (8.314 J/mol K). Equilibrium constant, $K_c$, can be calculated as:

$$K_c = \frac{C_{Ae}}{C_e} \quad (6)$$

where $C_{Ae}$ (mg/L) is the amount sorbed on solid at equilibrium. From the above equations, one gets:

$$\ln K_c = \frac{\Delta S^0}{R} - \frac{\Delta H^0}{RT} \quad (7)$$

The values of $\Delta H^0$ and $\Delta S^0$ were calculated from the slop and intercept of the plot between $\ln K_c$ versus $1/T$.

#### 2.4.4. Mixture of dyes—selectivity analysis

The obtained MIPs were brought into contact with a trichromatic mixture of reactive or basic dyes (30 mg/L of each dye). Immediately after mixing, the suspension was allowed to bind dyes by shaking for 24 h (at pH 10 for basic dyes and at pH 2 for reactive dyes). The temperature was maintained at 25 ± 1 °C. The same experiments were performed for the respective NIPs. Selectivity analysis has been also performed for real effluents, bearing the same reactive dyes, originating directly from the dyeing machine. The effluents were diluted to give approximately the same absorbance as the simulated effluents, for comparison reasons.

Usually, the static distribution coefficient $K_D$ (mL/g), the separation factor $\alpha$, and the relative separation factor $\beta$ are utilized to evaluate the molecular selectivity of MIPs. Parameters $K_D$, $\alpha$, and $\beta$ are defined as follows:

$$K_D = \frac{Q_e}{C_e} \quad (8)$$

The selectivity of one dye versus another is quantified by the ratio of the two partition coefficients $K_{D1}$ and $K_{D2}$ (for dyes 1 and 2, respectively):

$$\alpha = \frac{K_{D2}}{K_{D1}} \quad (9)$$

The higher value of $\alpha$, the better selectivity is; if $\alpha$ is close to 1.0, the sorbent has no selectivity.

$$\beta = \frac{\alpha_M}{\alpha_N} \quad (10)$$

where $\alpha_M$ and $\alpha_N$ are the distribution coefficients of MIPs and control polymers (NIPs), respectively. The relative separation factor $\beta$ demonstrates the difference between MIPs and NIPs. The higher value of $\beta$, the greater is the difference. When $\beta$ = 1.0, it means that there is no difference between MIPs and control polymers.

#### 2.4.5. Desorption experiments

Desorption of the sorbed RR and BR dyes from the imprinted polymers was studied in a batch experimental set-up. After adsorption, samples were collected and filtered using fixed pore-size membranes. Desorption experiments were performed by mixing the collected amount of loaded MIPs with aqueous solutions over a pH range of 2–12. After 24 h of shaking at 25 °C, samples were taken and analysis revealed the optimum desorption pH.

### 2.5. Analysis

The residual concentration of single dye solutions was calculated spectrophotometrically (UV–vis, model U-2000, Hitachi) at their respective $\lambda_{max}$. In the case of triple dye solutions, the absorbance $A$ was measured at the three wavelengths of maximum absorbance of dyes ($\lambda_{max,BR}$, $\lambda_{max,BB}$, $\lambda_{max,BY}$). The molar absorbtivity/extinction coefficients $E$ (L mol$^{-1}$ cm$^{-1}$) for the three dyes was calculated from the Lambert–Beer law [24]:

$$A = E \cdot Z \cdot C \quad (11)$$

where $Z$ the path length (cm). The resulting 3 × 3 equation system, expressed by Eqs. (11a)–(11c), can give the residual concentration of each dye:

$$A_{\lambda_1} = E_{\lambda_1,BY} \cdot Z \cdot C_{BY} + E_{\lambda_1,BB} \cdot Z \cdot C_{BB} + E_{\lambda_1,BR} \cdot Z \cdot C_{BR} \quad (11a)$$

$$A_{\lambda_2} = E_{\lambda_2,BY} \cdot Z \cdot C_{BY} + E_{\lambda_2,BB} \cdot Z \cdot C_{BB} + E_{\lambda_2,BR} \cdot Z \cdot C_{BR} \quad (11b)$$

$$A_{\lambda_3} = E_{\lambda_3,BY} \cdot Z \cdot C_{BY} + E_{\lambda_3,BB} \cdot Z \cdot C_{BB} + E_{\lambda_3,BR} \cdot Z \cdot C_{BR} \quad (11c)$$

where $A_{\lambda_1}$, $A_{\lambda_2}$, and $A_{\lambda_3}$ are the absorbencies of the mixture at the maximum wavelength of BY dye ($\lambda_1$ = 440 nm), BR ($\lambda_2$ = 488 nm), and BB ($\lambda_3$ = 607 nm), respectively. $E_{\lambda_1,BY}$, $E_{\lambda_1,BB}$, $E_{\lambda_1,BR}$ the absorbance coefficients of pure BY, BB, BR at the maximum wavelength of BY dye. $E_{\lambda_2,BY}$, $E_{\lambda_2,BB}$, $E_{\lambda_2,BR}$ the absorbance coefficients of pure BY, BB, BR at the maximum wavelength of BR dye. $E_{\lambda_3,BY}$, $E_{\lambda_3,BB}$, $E_{\lambda_3,BR}$ the absorbance coefficients of pure BY, BB, BR at the maximum wavelength of BB dye. The same procedure was followed for reactive dyes mixture. The effect of pH over both the calibration curves and the determined $\lambda_{max}$ wavelength of each dye were studied, but no significant deviation was observed.

## 3. Results and discussion

### 3.1. Choice of reagents

Typically, the generation of stable high affinity MIPs requires the following: (i) one or more functional monomers capable of forming stable complexes with the template molecule; (ii) high nominal cross-linking level for preserving the templated sites; (iii) the use of an aprotic apolar solvent as porogen [14]. However, these requirements are to some extent contradictory to the approaches available to incorporate hydrophilic surface properties: (i) polar porogens can be used. These solvate the polar functional groups of the monomers leaving them exposed at the pore walls after porogen removal; (ii) hydrophilic co-monomers or cross-linkers, e.g. MBA; (iii) postgrafting of hydrophilic chains can be employed [14].

The preparation of hydrophilic RR-MIP was guided by the sulfonate groups of reactive dye (R–$SO_3^-$) necessitated the interaction with a monomer, which could bear positive charged groups; e.g. –$NH_3^+$ in low pH values. Therefore, acrylamide (AAm) was selected as monomer which generates the hydrophilic surface of poly (acrylamide). Moreover the used cross-linker (MBA) is also hydrophilic, thus improving wetting by water. In the same manner, the preparation of hydrophilic BR-MIP was driven by the cationic groups of the basic dye ($N^+$), which had to interact with an opposite charged group of a monomer (e.g. R–$COO^-$), in order to take place a strong interaction to stabilize the prepared BR-MIP. Thus, the hydrophilic methacrylic acid was selected as monomer, which can strongly and ionically interact with the cationic group of the dye.

### 3.2. Characterization

Fig. 1a and b present the surface morphology of RR-MIP and BR-MIP after template extraction. It is readily observed that the BR-MIP is stiffer and scraggy, presenting numerous of cavities created after template extraction. This happens because of the different porogen used; BR-MIP was prepared with a non-polar solvent (DMF), while RR-MIP with water (high-polar solvent). In both MIPs, nano-sized particles were formed, which sequentially were aggregated into larger particles with cavities into the polymeric matrix. The surface area was determined to 112 and 98 m$^2$/g for BR-MIP and RR-MIP, respectively; close to the range of imprinted polymers [25,26]. In general, polymers made in "poor" solvents tend to have lower surface area than polymers made in "good" solvents as DMF [13,27].

Although imprinting synthesis has proven to be the most efficient method for tailoring binding sites, site accessibility remains a

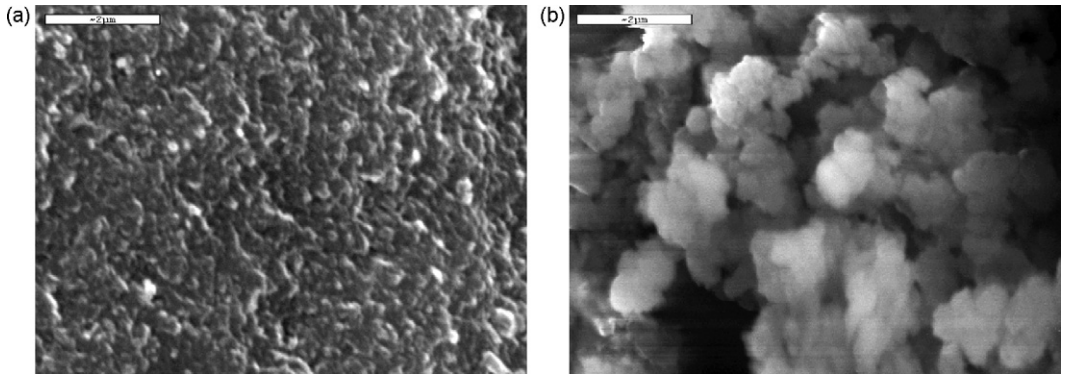


**Fig. 1.** SEM micrographs of MIPs after template extraction: (a) RR-MIP; (b) BR-MIP.

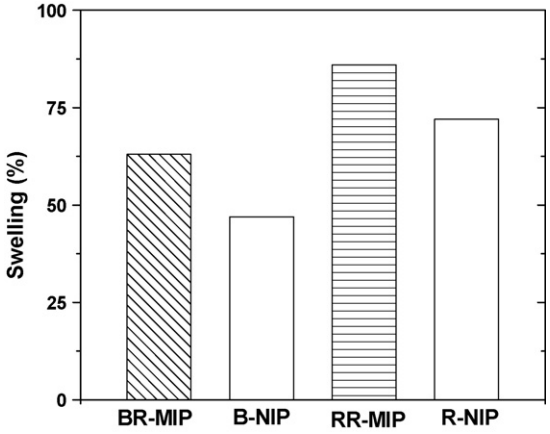


**Fig. 2.** Swelling ratios of the prepared MIPs and NIPs. (volume = 0.05 L; pH 2 for RR-MIP, R-NIP and pH 10 for BR-MIP, B-NIP; sorbent (MIPs, NIPs) = 0.5 g; contact time = 24 h; agitation speed 160 rpm; temperature = 25 °C).

problematic issue. The imprinted cavities located on the surface of the fine particles are fully accessible. However, those located inside the particles are only partially accessible or inaccessible, depending on the porosities of the corresponding hosts. Site accessibility is significantly improved by producing porous MIPs. In general, higher surface area presents advantages of perfect binding-site integrity, fully accessibility of imprinted sites, excellent mass transport and finely adjusted hydrodynamic properties [28].

Fig. 2 presents the swelling degrees of the prepared MIPs and NIPs (63% for BR-MIP, 86% for RR-MIP, 47% for B-NIP, and 72% for R-NIP). Lower swelling means that the recognition sites are fixed more rigid on the polymer surface. The higher swelling of RR-MIP and R-NIP is attributed to their more hydrophilic character.

In general, to combat swelling, most imprinted systems will incorporate adequate ratios of cross-linkers into the backbone [27]. It has been communicated that: (i) MIPs prepared with low ratio of cross-linking (2 mmol monomer/5 mmol cross-linker) give cavities too close to each other, creating a larger but less recognitive pore; (ii) MIPs prepared with high cross-linking ratio (2 mmol monomer/20 mmol cross-linker), hindered the diffusion of template into the polymeric matrix [27]. In our study, to give rigidity to the functional cavities and to allow recognition, a medium ratio of cross-linking was used (2 mmol monomer/10 mmol cross-linker).

### 3.3. Effect of pH (pH-edges)

One of the most important parameters controlling the dye adsorption process is pH, because it could influence the properties of the sorbent as well as sorbate speciation. Fig. 3a shows the experimental results of dye removal by MIPs under various constant pH values. Data for BR-MIP reveal that the adsorption was better in basic conditions (high pH values) than in acidic ones; the higher dye removal was achieved at pH 10 (69%). Contrarily, RR-MIP presents better rebinding in acidic environment (66% at pH 2). Fig. 3b presents the effects of pH on desorption of dye from MIPs. BR-MIP desorbed about 91% at pH 2 (acidic conditions), while 3% at pH 12 (alkaline conditions). Thus, decreasing the pH of eluent, an increase of desorption was observed. In contrast, RR-MIP at pH 10 presented the highest desorption ratio (88%) and at pH 2 the lowest one (8%). Therefore, the exact opposite trend of the adsorption process with pH was followed in desorption.

### 3.4. Kinetics

The behaviour of sorbents on the adsorption kinetics is depicted in Fig. 4. A monotonous decreasing trend with high rates at the beginning of adsorption observed for both the prepared dye-MIPs, whereas the initial step descent is followed by a flat plateau (saturation values). Equilibrium has been almost reached within 4 h for both MIPs. In general, adsorption of dye was quite fast due to high complexation rate into the MIP structure. If equilibrium is achieved within 3 h, the process is usually kinetic controlled and above 24 h, it is diffusion controlled. Either or both kinetic and adsorption processes may be rate controlled in the 3–24 h period [19]. The intraparticle diffusion model, presented as inset in Fig. 4, succeeded in predicting the experimental data. All data analysis was performed using nonlinear least-square fitting. A Levenberg–Marquardt algorithm was used to iteratively search for the parameters that best fit the data, determined by minimization of the $\chi^2$ value [29].The resulted diffusion coefficients for BR-MIPs and RR-MIPs were $4.99 \times 10^{-13}$ m$^2$/s and $5.08 \times 10^{-13}$ m$^2$/s, respectively.

### 3.5. Equilibrium—thermodynamics

The adsorption isotherms are depicted in Fig. 5a–c for RR-MIP, BR-MIP and NIP, respectively. Experimental data were fitted by the Freundlich model and the resulting parameters are given in Table 2. The correlation coefficient ($R^2 \approx 0.998$) reveals that the particular isotherm provides adequate theoretical correlation. Data showed an increase in the amount of dye sorbed when the initial dye concentration was increased. One may discern that there is an increase in the adsorption capacity as temperature was increased, for Fig. 5a and b. Yan et al. [12] showed that the maximum adsorption capacity for MIPs with malachite green (basic dye) as template molecule was 2.33 μmol/g (=0.85 mg/g). In our study, the adsorption-loading

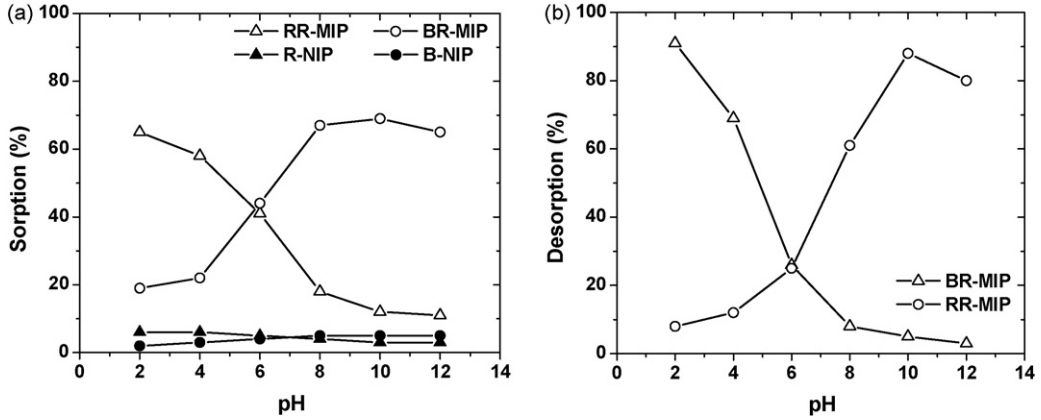


**Fig. 3.** (a) Effect of pH on the sorption of RR and BR onto RR-MIP and BR-MIP, respectively. (b) Effect of pH on desorption of RR and BR from RR-MIP and BR-MIP, respectively (initial concentartion = 100 mg/L; volume = 0.05 L; sorbent (MIPs, NIPs) = 0.5 g; contact time = 24 h; agitation speed 160 rpm; temperature = 25 °C).

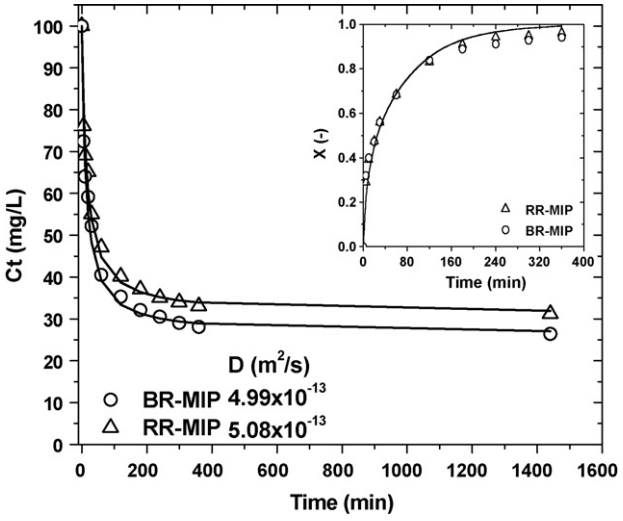


**Fig. 4.** Adsorption kinetic data for BR-MIP and RR-MIP. Inset: intraparticle diffusion model fitted to the kinetic data (initial concentration = 100 mg/L; volume = 0.05 L; sorbent (MIPs) = 0.5 g; contact time = 24 h; agitation speed 160 rpm; temperature = 25 °C).

values of dye-MIPs reach up to 12.31 mg/g; that is 15 times greater.

The values of $\Delta H^0$ and $\Delta S^0$ were calculated from the slop and intercept of the plot between $\ln K_c$ versus $1/T$ ($R^2 > 0.989$, data not shown). All thermodynamic parameters, at selected concentrations and all temperatures are given in Table 3 for RR and in Table 4 for BR. The positive values of $\Delta H^0$ suggest the endothermic nature of the process. The negative values of $\Delta G^0$ suggest that the process is spontaneous with high preference for dye molecules. Since the adsorption is endothermic, the amount sorbed at equilibrium is increased with increasing temperature. The positive values of $\Delta S^0$ show the increased randomness at the solid/liquid interface. During the adsorption the coordinated water molecules that are displaced by the dye molecules gain more translational entropy, than is lost by the dye molecules, resulting in increased randomness in the dye-MIPs interaction [30].

**Table 2**
Equilibrium constants for the adsorption of dyes (RR and BR) onto MIPs and NIPs.

| Sorbent | Freundlich model | | | |
|---|---|---|---|---|
| | $T$ (K) | $K_F$ ($mg^{1-n}$ $L^n/g$) | $n$ | $R^2$ |
| RR-MIP | 298 | 1.246 | 0.489 | 0.998 |
| | 318 | 1.380 | 0.488 | 0.996 |
| | 338 | 1.593 | 0.472 | 0.998 |
| BR-MIP | 298 | 1.765 | 0.460 | 0.983 |
| | 318 | 1.897 | 0.443 | 0.986 |
| | 338 | 2.027 | 0.437 | 0.988 |
| R-NIP | 298 | 0.130 | 0.232 | 0.990 |
| B-NIP | 298 | 0.142 | 0.262 | 0.978 |

The thermodynamic parameters ($\Delta H^0$, $\Delta S^0$) showed a decrease with increasing initial concentration and amount sorbed. This effect could be attributed to: (i) the energetic heterogeneity of the surface and (ii) to dye–dye interactions. The dependence of heat of adsorption with surface coverage is usually observed to display the sorbent–sorbate interactions followed by sorbate–sorbate interactions [31]. Exactly the same trend has been reported for the adsorption of methylene blue by diatomaceous silica [32]. At low concentrations, hence at low $Q_e$, the adsorption sites having the highest affinity for dyes are occupied first. Then, with increasing $Q_e$, the remaining sites with lower affinity are progressively occupied. The variation of heat of adsorption with surface loading can also be attributed to the possibility of lateral interactions between dye molecules. It is well known that ionic dyes tend to aggregate in dilute solutions, leading to dimmer formation [33]. It is supposed that dimmer formation in solution is mainly due to hydrophobic interactions or permanent and transition dipole moments [33,34]. Although dyes are very individualistic as structure, certain broad rules are well established regarding their dimerization. The probability increases with an increase of dye concentration or ionic strength; it will decrease with temperature rising or organic solvents adding [33].

### 3.6. Regenerability

The repeated use of the sorbent (regenerability), which is a key factor in improving wastewater process economics, was estimated in four sequential cycles of adsorption–desorption (Fig. 6). The loss in the adsorption capacity between the first and the last cycle was approximately 10% for both MIPs. This gives evidence that the prepared materials can be used repeatedly without loosing significantly their adsorption capacities.

### 3.7. Adsorption/rebinding mechanism

To shed light in the adsorption mechanism, the surface charge of the prepared materials was estimated versus pH (Fig. 7). The

**Table 3**
Thermodynamic parameters for the adsorption of RR onto RR-MIP.

| $C_0$ (mg/L) | Temperature (K) | $Q_e$ (mg/g) | $K_c$ | $\Delta G^0$ (kJ/mol) | $\Delta H^0$ (kJ/mol) | $\Delta S^0$ (J/mol K) |
|---|---|---|---|---|---|---|
| 10 | 298 | 0.92 | 11.35 | −6.02 | | 56.40 |
| | 318 | 0.94 | 14.87 | −7.14 | 10.79 | 56.37 |
| | 338 | 0.95 | 19.00 | −8.27 | | 56.40 |
| 100 | 298 | 6.90 | 2.23 | −1.98 | | 28.33 |
| | 318 | 7.20 | 2.57 | −2.50 | 6.46 | 28.17 |
| | 338 | 7.50 | 3.00 | −3.09 | | 28.25 |
| 200 | 298 | 11.00 | 1.22 | −0.50 | | 18.14 |
| | 318 | 11.60 | 1.38 | −0.85 | 4.91 | 18.12 |
| | 338 | 12.19 | 1.56 | −1.26 | | 18.25 |

resulted $pH_{zpc}$ for the BR-MIP and RR-MIP were 3.27 and 4.65, respectively.

For the case of BR-MIP, where the adsorption was realized at pH 10, the rebinding could be succeeded through strong ionic interactions between the negative charged MIP ($pH > pH_{zpc}$) and the dye molecule. The basic dye, as a quaternary ammonium salt, exists as a permanent cation resulting an attraction between the cationic groups of the dye ($N^+$) with the negatively charged carboxyl groups ($R–COO^-$) of the MAA. For RR-MIP, the rebinding was carried out at pH 2 and could be achieved through high-affinity electrostatic interactions between the positive charged MIP ($pH < pH_{zpc}$) and the dye molecule. Specifically, the protonated amino groups of acrylamide ($NH_3^+$) interact strongly at pH 2 with the sulfonate groups of dye (Eq. (12)):

$$R_1–SO_3^- + R_2–CO–NH_3^+ \leftrightarrow R_2–CO–NH_3\cdots O_3S–R_1 \quad (12)$$

The $pK_a$ of the sulphate groups of the reactive dye are in the range 0.54–1.44, according to the SPARC software model v.4.2 (licensed by EPA, USA) [35], which means that there is a great percentage of the dye molecule in the anionic form (deprotonated) at pH 2.

All the aforementioned interactions can be affirmed by the infrared spectra of the loaded MIPs (BR-MIP and RR-MIP) along with the respective NIPs and single dyes, which are presented in Fig. 8. In the case of BR dye, four characteristic peaks were presented; the tertiary amino C–N stretch bond at 1136 $cm^{-1}$, the nitrate group at 1354 $cm^{-1}$, the open-chain azo group (–N=N–) at 1574 $cm^{-1}$, and the aromatic ring stretch at 1601 $cm^{-1}$. The strong ionic interactions between the negatively charged carboxylic groups and the positively charged dye molecules are revealed by the shift of the peak from 1661 $cm^{-1}$ in B-NIPs to 1653 $cm^{-1}$ in BR-MIPs. The latter is attributed to the asymmetric deformation of the carboxyl ion of the methacrylic acid. Apart from this, the absence of the peak at 1574 $cm^{-1}$ (–N=N–) in the B-NIP spectrum, affirmed the structural difference between MIPs and NIPs, that is the absence of the dye template in the non-imprinted polymer. On the other hand, RR dye presents the peak of azo groups at 1621 $cm^{-1}$, the strong peak at 1149 $cm^{-1}$ because of the sulfate ion ($–SO_3^-$) and the C–Cl stretch at 771 $cm^{-1}$. In addition, the strong electrostatic interactions between sulfonate groups of the dye and protonated amide groups of the acrylamide were presented through the shift of the peak from 1691 $cm^{-1}$ in R-NIP to 1682 $cm^{-1}$ in RR-MIP.

For sorbent motivated adsorption three loosely defined categories are traditionally distinguished: (i) chemical, or chemisorption, involves solute–sorbent interactions having the characteristics of true chemical bonds; (ii) electrostatic adsorption which involves electrostatic bonds and (iii) physical adsorption, or physisorption, resulting from the action of van der Waals forces [36]. Taking into account: (i) the previous classification; (ii) the reversibility of the process; (iii) FTIR analysis and (iv) the applicability of Freundlich isotherm [37], which does not describe chemical adsorption, one can postulate that the main adsorption mechanism is electrostatic adsorption. Additionally, a limited adsorption due to dye-polymer hydrophobic effect could also contribute given the small adsorption of dyes by NIPs [38].

### 3.8. Selectivity studies for simulated effluents

Table 5 shows the experimental results from the adsorption experiments in trichromatic dye solutions. The prepared basic and reactive dye-MIPs sorb with extreme selectivity its template molecule from a trichromatic dye solution, presenting very high distribution coefficients. The simultaneous adsorption of small amounts of the other competitive dyes (although several dyes had smaller size than the target molecules) could be attributed to the electrostatic attractions developed between MIPs and the dye molecules in a non-specific manner [13]. The calculation of the relative separation factors ($\beta$) of BR-MIP and RR-MIP showed that the imprinted matrix for BR/BB, BR/BY, RR/RB, RR/RY was approximately 63, 67, 39, and 40 times greater than non-imprinted matrix, respectively. Therefore, the selectivity of MIPs against their respective control polymers is doubtless and definite.

**Table 4**
Thermodynamic parameters for the adsorption of BR onto BR-MIP.

| $C_0$ (mg/L) | Temperature (K) | $Q_e$ (mg/g) | $K_c$ | $\Delta G^0$ (kJ/mol) | $\Delta H^0$ (kJ/mol) | $\Delta S^0$ (J/mol K) |
|---|---|---|---|---|---|---|
| 10 | 298 | 0.95 | 18.23 | −7.19 | | 66.62 |
| | 318 | 0.96 | 23.39 | −8.33 | 12.66 | 66.02 |
| | 338 | 0.97 | 33.48 | −9.87 | | 66.64 |
| 100 | 298 | 7.49 | 2.98 | −2.71 | | 27.44 |
| | 318 | 7.70 | 3.35 | −3.19 | 5.47 | 27.25 |
| | 338 | 7.95 | 3.88 | −3.81 | | 27.45 |
| 200 | 298 | 12.28 | 1.60 | −1.16 | | 18.86 |
| | 318 | 12.80 | 1.78 | −1.52 | 4.46 | 18.81 |
| | 338 | 13.40 | 2.03 | −1.99 | | 19.08 |

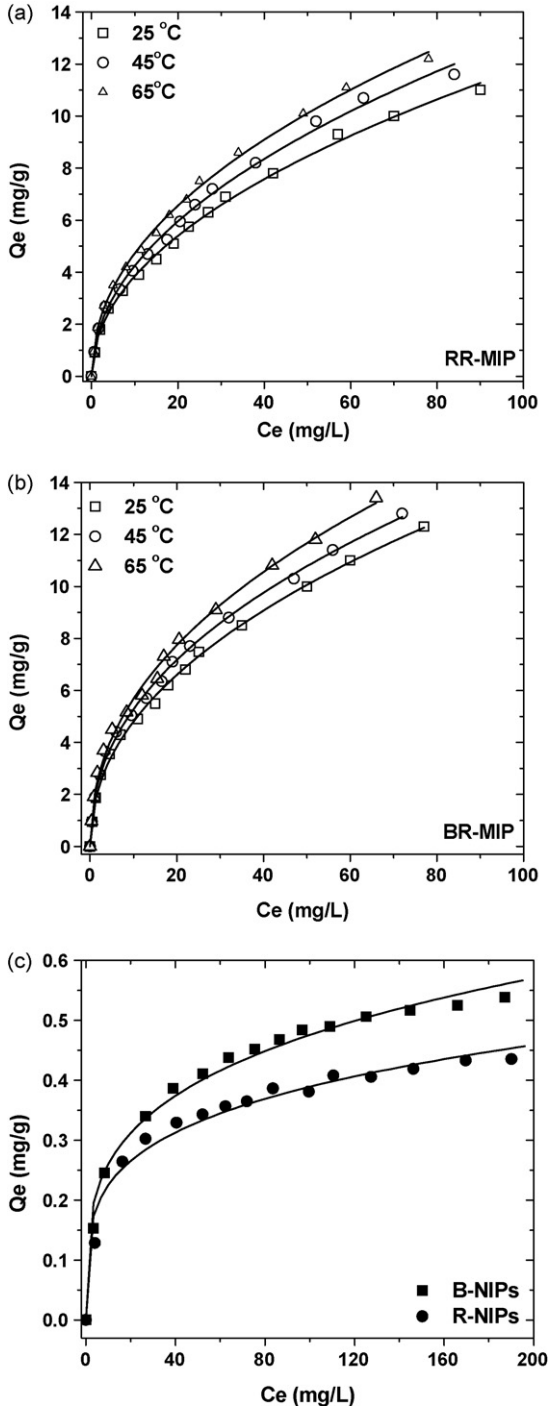


**Fig. 5.** Adsorption/binding isotherms, fitted to the Freundlich model, for: (a) RR-MIP; (b) BR-MIP and (c) NIPs (initial concentartion = 10–200 mg/L; volume = 0.05 L; sorbent (MIPs) = 0.5 g; contact time = 24 h; agitation speed 160 rpm; temperature = 25 °C).

### 3.9. Selectivity studies for real effluents

Table 5 presents the selectivity parameters for real effluent bearing the same reactive dyes. Comparing with the respective simulated, it seems that there is a reduction in $K_D \sim 24\%$. Reactive dyebath effluents comprise a variety of dye auxiliaries such as NaCl (20–40 g/L), $Na_2CO_3$ (5–15 g/L), sequestering and organic agents [39]. The inorganic auxiliaries increase the ionic strength of the solution and causes dye dimerization with a consequent

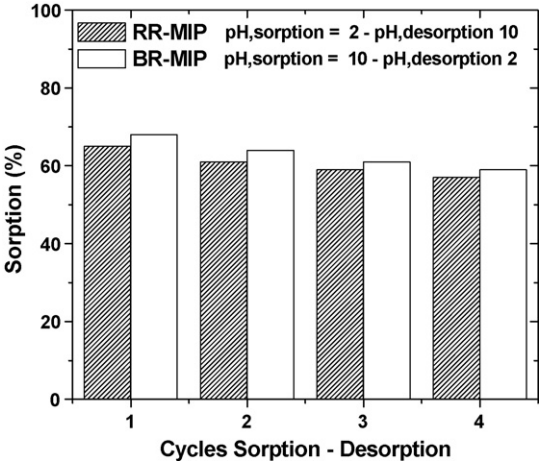


**Fig. 6.** Adsorption–desorption cycles for BR-MIP and RR-MIP.

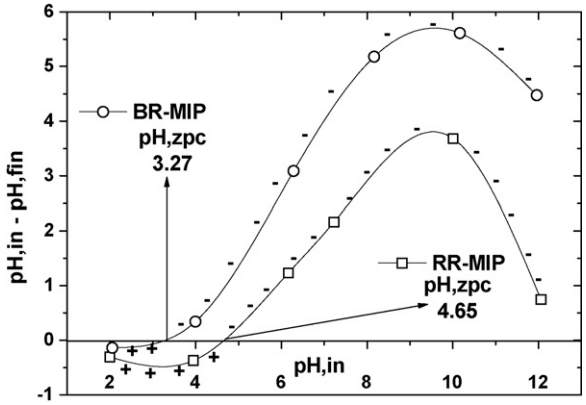


**Fig. 7.** Determination of the $pH_{zpc}$ by the solid addition method.

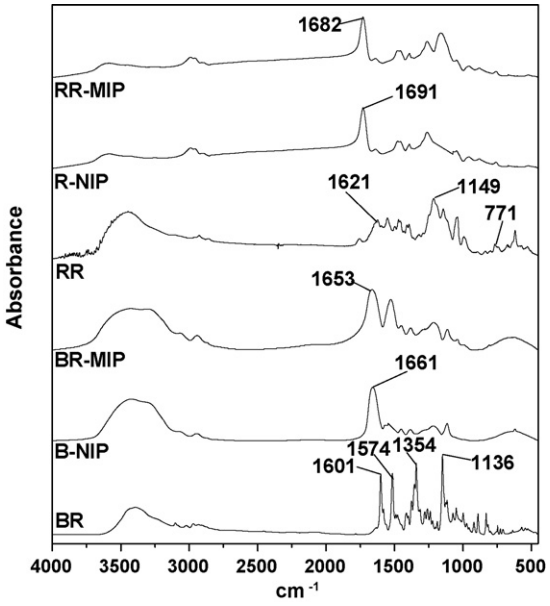


**Fig. 8.** FTIR spectra of the prepared BR-MIP, RR-MIP, the respective NIPs, and the dyes.

**Table 5**
Molecular selectivity of the prepared MIPs/NIPs in trichromatic dye solution.

| $K_D$ (L/g) | | | | | | | |
|---|---|---|---|---|---|---|---|
| Sorbent | BR | BB | BY | $\alpha_1 = K_{D_{BR}}/K_{D_{BB}}$ | $\alpha_2 = K_{D_{BR}}/K_{D_{BY}}$ | $\beta_1 = \alpha_{1,MIP}/\alpha_{1,NIP}$ | $\beta_2 = \alpha_{2,MIP}/\alpha_{2,NIP}$ |
| Simulated basic dye effluent | | | | | | | |
| BR-MIP | 1.100 | 0.016 | 0.015 | 67.57 | 74.71 | 63.15 | 67.31 |
| B-NIP | 0.013 | 0.012 | 0.011 | 1.07 | 1.11 | – | – |
| | RR | RB | RY | $\alpha_3 = K_{D_{RR}}/K_{D_{RB}}$ | $\alpha_4 = K_{D_{RR}}/K_{D_{RY}}$ | $\beta_3 = \alpha_{3,MIP}/\alpha_{3,NIP}$ | $\beta_4 = \alpha_{4,MIP}/\alpha_{4,NIP}$ |
| Simulated reactive dye effluent | | | | | | | |
| RR-MIP | 0.650 | 0.015 | 0.014 | 43.5 | 46.21 | 39.18 | 40.18 |
| R-NIP | 0.013 | 0.011 | 0.011 | 1.11 | 1.15 | – | – |
| | RR | RB | RY | $\alpha'_3 = K_{D_{RR}}/K_{D_{RB}}$ | $\alpha'_4 = K_{D_{RR}}/K_{D_{RY}}$ | $\beta'_3 = \alpha'_{3,MIP}/\alpha'_{3,NIP}$ | $\beta'_4 = \alpha'_{4,MIP}/\alpha'_{4,NIP}$ |
| Real reactive dye effluent | | | | | | | |
| RR-MIP | 0.488 | 0.011 | 0.010 | 42.81 | 47.84 | 37.22 | 39.87 |
| R-NIP | 0.010 | 0.009 | 0.008 | 1.15 | 1.20 | – | – |

hindered access in the active sites of MIPs. The organic auxiliaries could be partially bound onto MIPs surface by hydrophobic interactions limiting the access to the target dye molecule. However, no significant reduction was observed in the partition coefficients and separation factors which indicate that the process remains selective.

## 4. Conclusions

In the present investigation, water-compatible MIPs were prepared and evaluated as sorbents for basic (BR-MIP) and reactive dyes (RR-MIPs). The experimental observations are summarized below:

- The BR-MIP was prepared in organic medium while RR-MIP in aqueous. Both of them presented relatively low swelling percentage (63–86%).
- The optimum condition for adsorption experiments was found to be pH 2 for BR-MIP while pH 10 for RR-MIP. Effective diffusion coefficients were found to be at the order $5 \times 10^{-13}$ m$^2$/s. Desorption of loaded BR-MIP (91%) succeeded at pH 2, while for the respective RR-MIP (88%) at pH 10.
- Equilibrium data were successfully fitted to the Freundlich isotherm. The maximum adsorption loading, under the studied experimental conditions, found to be about 12 mg/g for both MIPs.
- MIPs were applied in four sequential cycles of adsorption–desorption with a limited loss of adsorption capacity, only 10%.
- The proposed rebinding mechanism (hydrogen bonding–electrostatic interactions) is affirmed by the shift of the carbonyl peak from NIPs to MIPs. Thermodynamic analysis showed the endothermic and spontaneous nature of the process, which could be characterized as electrostatic adsorption.
- Selectivity studies with simulated effluents showed that MIPs were selective to their template molecules presenting high distribution coefficients (0.650–1.100 L/g) and high separation factors (40–75).
- Selectivity studies, with diluted real effluents, showed ~24% reduction in distribution coefficient but with the same high separation factors. The latter indicates that MIPs could be employed for practical use. However, the next step would be preparation of MIPs with higher adsorption capacity in order to become more attractive in large-scale implementations.

## Acknowledgements

The authors are grateful for this study to the Greek Ministry of Development through the Greek–German Bilateral Corporation for the financial support (project No. GSRT 107-c).

## References

[1] F.H. Dickey, Specific adsorption, J. Phys. Chem. 59 (1955) 695–707.
[2] G. Wulf, A. Sarhan, Use of polymers with enzyme-analogous structures for the resolution of racemates, Angew. Chem. Int. Ed. Engl. 11 (1972) 341–344.
[3] T. Takeuchi, D. Fukuma, J. Matsui, Combinatorial molecular imprinting: an approach to synthetic polymer receptors, Anal. Chem. 71 (1999) 285–290.
[4] C. Yu, K. Mosbach, Molecular imprinting utilizing an amide functional group for hydrogen bonding leading to highly efficient polymers, J. Org. Chem. 62 (1997) 4057–4064.
[5] S.A. Piletsky, T.L. Panasyuk, E.V. Piletskaya, I.A. Nicholls, M. Ulbricht, Receptor and transport properties of imprinted polymer membranes—a review, J. Membr. Sci. 157 (1999) 263–278.
[6] S.A. Piletsky, A. Alcock, A.P.F. Turner, Molecular imprinting: at the edge of the third millennium, Trends Biotechnol. 19 (2001) 9–12.
[7] G. Crini, Recent developments in polysaccharide-based materials used as adsorbents in wastewater treatment, Prog. Polym. Sci. 30 (2005) 38–70.
[8] T. Robinson, G. McMullan, R. Marchant, P. Nigam, Remediation of dyes in textile effluent: a critical review on current treatment technologies with a proposed alternative, Bioresour. Technol. 77 (2001) 247–255.
[9] N.R. Salaskar, A.S. Sahasrabudhe, Development of shades on cellulosic substrates with trichromatic reactive dyes using CCM technique, BTRA 33 (2003) 19–26.
[10] R.S. Blackburn, Natural polysaccharides and their interaction with dye molecules: applications in effluent treatment, Environ. Sci. Technol. 38 (2004) 4905–4909.
[11] G.Z. Kyzas, D.N. Bikiaris, N.K. Lazaridis, Low-swelling chitosan derivatives as biosorbents for basic dyes, Langmuir 24 (2008) 4791–4799.
[12] S. Yan, Z. Gao, Y. Fang, Y. Cheng, H. Zhou, H. Wang, Characterization and quality assessment of binding properties of malachite green molecularly imprinted polymers prepared by precipitation polymerization in acetonitrile, Dyes Pigments 74 (2007) 572–577.
[13] E.V. Piletska, A.R. Guerreiro, M. Romero-Guerra, I. Chianella, A.P.F. Turner, S.A. Piletsky, Design of molecular imprinted polymers compatible with aqueous environment, Anal. Chim. Acta 607 (2008) 54–60.
[14] B. Dirion, Z. Cobb, E. Schillinger, L.I. Andersson, B. Sellergren, Water-compatible molecularly imprinted polymers obtained via high-throughput synthesis and experimental design, J. Am. Chem. Soc. 125 (2003) 15101–15109.
[15] M. Sibrian–Vazquez, D.A. Spivak, Enhanced enantioselectivity of molecularly imprinted polymers formulated with novel cross-linking monomers, Macromolecules 36 (2003) 5105–5113.
[16] A.G. Mayes, M.J. Whitcombe, Synthetic strategies for the generation of molecularly imprinted organic polymers, Adv. Drug Deliv. Rev. 57 (2005) 1742–1778.
[17] L.S. Balistrieri, J.W. Murray, The surface chemistry of goethite (αFeOOH) in major ion seawater, Am. J. Sci. 281 (1981) 788–806.
[18] R.L. Tseng, S.K. Tseng, Pore structure and adsorption performance of the KOH-activated carbons prepared from corncob, J. Colloid Interf. Sci. 287 (2005) 428–437.
[19] Y.S. Ho, J.C.Y. Ng, G. McKay, Kinetics of pollutant sorption by biosorbents: review, Sep. Purif. Methods 29 (2000) 189–232.

[20] A.M. Rampey, R.J. Umpleby II, G.T. Rushton, J.C. Iseman, R.N. Shah, K.D. Shimizu, Characterization of the imprint effect and the influence of imprinting conditions on affinity, capacity, and heterogeneity in molecularly imprinted polymers using the Freundlich isotherm-affinity distribution analysis, Anal. Chem. 76 (2004) 1123–1133.
[21] H.M.F. Freundlich, Über die adsorption in lösungen (adsorption in solution), Z. Phys. Chem. 57 (1906) 384–470.
[22] R.P. Schwarzenbach, P.M. Cschwend, D.M. Imboden, Environmental Organic Chemistry, John Wiley & Sons, NY, 1993.
[23] J.M. Smith, H.C. Van Ness, Introduction to Chemical Engineering Thermodynamics, 4th ed., McGraw-Hill, Singapore, 1987.
[24] A. Beer, Bestimmung der absorption des rothen lichts in farbigen flussigketiten, Ann. Phys. Chem. 86 (1852) 78–88.
[25] P. Dzygiel, E. O'Donnell, D. Fraier, C. Chassaing, P.A.G. Cormack, Evaluation of water-compatible molecularly imprinted polymers as solid-phase extraction sorbents for the selective extraction of sildenafil and its desmethyl metabolite from plasma samples, J. Chromatogr. B 853 (2007) 346–353.
[26] M.-J. Syu, J.-H. Deng, Y.-M. Nian, Towards bilirubin imprinted poly(methacrylic acid-*co*-ethylene glycol dimethylacrylate) for the specific binding of α-bilirubin, Anal. Chim. Acta 504 (2004) 167–177.
[27] N.M. Bergmann, N.A. Peppas, Molecularly imprinted polymers with specific recognition for macromolecules and proteins, Prog. Polym. Sci. 33 (2008) 271–288.
[28] S. Dai, Z. Zhang, C. Liang, Hierarchically imprinted nanostructures for separation of metal ions, in: J.A. Schwarz, C.I. Contescu, K. Putyera (Eds.), Dekker Encyclopedia of Nanoscience and Nanotechnology, CRC Press, 2004.
[29] D.W. Marquardt, An algorithm for least-squares estimation of nonlinear parameters, J. Soc. Ind. Appl. Mat. 11 (1963) 431–441.
[30] M.R. Unnithan, T.S. Anirudhan, The kinetics and thermodynamics of sorption of chromium(VI) onto the iron(III) complex of a carboxylated polyacrylamide-grafted sawdust, Ind. Eng. Chem. Res. 40 (2001) 2693–2701.
[31] V.C. Srivastava, I.D. Mall, I.M. Mishra, Adsorption thermodynamics and isosteric heat of adsorption of toxic metal ions onto bagasse fly ash (BFA) and rice husk ash (RHA), Chem. Eng. J. 132 (2007) 267–278.
[32] Z. Al-Qodah, W.K. Lafi, Z. Al-Anber, M. Al-Shannag, A. Harahsheh, Adsorption of methylene blue by acid and heat treated diatomaceous silica, Desalination 217 (2007) 212–224.
[33] A. Niazi, A. Yazdanipour, J. Ghasemi, M. Kubista, Spectrophotometric and thermodynamic study on the dimerization equilibrium of ionic dyes in water by chemometrics method, Spectrochim. Acta Part A 65 (2006) 73–78.
[34] K. Murakami, Thermodynamic and kinetic aspects of self-association of dyes in aqueous solution, Dyes Pigments 53 (2002) 31–43.
[35] S.H. Hilal, S.W. Karickhoff, L.A. Carreira, Prediction of chemical reactivity parameters and physical properties of organic compounds from molecular structure using SPARC, U.S. Environmental Protection Agency, Publication No. EPA/600/R-03/030, Athens, GA, 2003, p. 158.
[36] W.J. Weber Jr., F.A. Digiano, Process Dynamics in Environmental Systems, John Wiley & Sons, NY, 1996.
[37] D.G. Kinniburgh, General purpose adsorption isotherms, Environ. Sci. Technol. 20 (1986) 895–904.
[38] A.T. Slark, P.M. Hadgett, The effect of polymer structure on specific interactions between dye solutes and polymers, Polymer 40 (1999) 1325–1332.
[39] I. Kabdaşli, B. Vardar, I. Arslan-Alaton, O. Tünay, Effect of dye auxiliaries on color and COD removal from simulated reactive dyebath effluent by electrocoagulation, Chem. Eng. J. 148 (2009) 89–96.